

New physics in the weak interaction of $\bar{B} \rightarrow D^{(*)}\tau\bar{\nu}$

Minoru TANAKA* and Ryoutaro WATANABE†

Department of Physics, Graduate School of Science,

Osaka University, Toyonaka, Osaka 560-0043, Japan

Abstract

Recent experimental results on exclusive semi-tauonic B meson decays, $\bar{B} \rightarrow D^{(*)}\tau\bar{\nu}$, showing sizable deviations from the standard model prediction, suggest a new physics in which the structure of the relevant weak charged interaction may differ from that of the standard model. We study the exclusive semi-tauonic B decays in a model-independent manner using the most general set of four-Fermi interactions in order to clarify possible structures of the charged current in new physics. It turns out that correlations among observables including tau and D^* polarizations and q^2 distributions are useful to distinguish possible new physics operators. Further, we investigate some interesting models to exhibit the advantage of our model-independent analysis. As a result, we find that two Higgs doublet models without tree-level flavor changing neutral currents (FCNC) and the minimal supersymmetric standard model with R -parity violation are unlikely to explain the present experimental data, while two Higgs doublet models with FCNC and a leptoquark model are consistent with the data.

PACS numbers: 12.60.Fr, 13.20.-v, 13.20.He, 14.80.Sv

*Electronic address: tanaka@phys.sci.osaka-u.ac.jp

†Electronic address: ryoutaro@het.phys.sci.osaka-u.ac.jp

I. INTRODUCTION

The $V - A$ structure of the weak interaction was established in the study of nuclear β decays for the quarks and lepton in the first generation [1]. Since then, several charged current interactions in the second and third generations have been investigated and turned out to be described by similar $V - A$ interactions with a reasonable level of accuracy.

Among the charged current processes observed so far, pure- and semi- tauonic B meson decays, $\bar{B} \rightarrow \tau \bar{\nu}$ [2, 3] and $\bar{B} \rightarrow D^{(*)} \tau \bar{\nu}$ [4–8] are thought-provoking in the sense that they contain both the quark (b) and the lepton (τ) in the third generation. Their large masses suggest a close connection with the electroweak symmetry breaking (EWSB), which is still not fully understood even after the discovery of a di-gamma resonance [9, 10].

The EWSB sector in a candidate of new physics beyond the standard model (SM) often has a different structure from that of the SM. A typical example is the two Higgs doublet model (2HDM) of type II [11], which has the Higgs sector identical to that of the minimal supersymmetric standard model (MSSM) [12] at the tree level. A pair of charged Higgs bosons appears in this class of models, and its couplings to fermions are proportional to the involved fermion masses and further enhanced if the ratio of vacuum expectation values, $\tan \beta$, is large. Several authors have studied effects of these enhanced couplings, which modify the $V - A$ structure, in the pure- and semi- tauonic B decays [13–26].

From the experimental point of view, these B decay processes are rather difficult to identify because of two or more missing neutrinos in the final states. With the help of large statistics and low backgrounds, however, they are good targets of e^+e^- B factory experiments. The observed branching fraction of $\bar{B} \rightarrow \tau \bar{\nu}$ is $O(10^{-4})$ and that of $\bar{B} \rightarrow D^{(*)} \tau \bar{\nu}$ is $O(10^{-2})$. Comparing the pure- and semi- tauonic B decays, the latter provides a wide variety of observables besides the larger branching fraction, such as decay distributions [16, 20–24, 27–31] and polarizations [15, 25, 27, 29]. Hence, the semi-tauonic processes allow us to investigate the structure of the relevant charged current interaction, and we concentrate on $\bar{B} \rightarrow D^{(*)} \tau \bar{\nu}$ in this work.

Another advantage of $\bar{B} \rightarrow D^{(*)} \tau \bar{\nu}$ is that theoretical and experimental uncertainties tend to be reduced by taking the ratio of branching fraction to the semileptonic decays, $\bar{B} \rightarrow D^{(*)} \ell \bar{\nu}$, where ℓ denotes e or μ . These decay modes including lighter charged leptons are supposed to be less sensitive to the EWSB sector and assumed to be described by the

SM in the present work.

The ratios of the branching fractions are defined by

$$R(D^{(*)}) \equiv \frac{\mathcal{B}(\bar{B} \rightarrow D^{(*)} \tau^- \bar{\nu}_\tau)}{\mathcal{B}(\bar{B} \rightarrow D^{(*)} \ell^- \bar{\nu}_\ell)}, \quad (1)$$

and their experimental values are summarized as

$$R(D) = 0.42 \pm 0.06, \quad R(D^*) = 0.34 \pm 0.03, \quad (2)$$

where we combine the results of BaBar [5] and Belle [6–8] assuming the gaussian distribution. These measurements seem to be larger than the SM predictions,

$$R(D) = 0.305 \pm 0.012, \quad R(D^*) = 0.252 \pm 0.004, \quad (3)$$

and the SM is disfavored at 3.5σ .

Interestingly, as is shown in Ref. [5], one of $R(D)$ and $R(D^*)$ is made consistent with the corresponding experimental value in the 2HDM of type II by adjusting $\tan \beta/m_{H^\pm}$, but it is unlikely to make both of them agree with the experimental results. Thus, the 2HDM of type II is also disfavored.

In the present work, we first provide a model-independent framework for the semi-tauonic B decays in order to clarify the type of new physics that is required to explain the current experimental results. Then, we apply the framework to analyzing several models. The rest of this paper is organized as follows: In Sec. II, we present the most general effective Lagrangian of $b \rightarrow c \tau \bar{\nu}$ and the resultant helicity amplitudes of $\bar{B} \rightarrow D^{(*)} \tau \bar{\nu}$. Experimental constraints and theoretical predictions are given in Sec. III. We discuss how to distinguish new physics contributions that appear in the effective Lagrangian in Sec. IV. We analyze 2HDMs, MSSM with R -parity violation and a leptoquark model in Sec. V. Section VI is devoted to our conclusions.

II. EFFECTIVE LAGRANGIAN AND HELICITY AMPLITUDES

A. Effective Lagrangian for $b \rightarrow c \tau \bar{\nu}$

The semi-tauonic bottom quark decay, $b \rightarrow c \tau \bar{\nu}$, is described by the four-Fermi interaction of charged left-handed currents in the SM. Other four-Fermi operators might be induced in the presence of new physics.

The effective Lagrangian that contains all conceivable four-Fermi operators is written as

$$-\mathcal{L}_{\text{eff}} = 2\sqrt{2}G_F V_{cb} \sum_{l=e,\mu,\tau} [(\delta_{l\tau} + C_{V_1}^l)\mathcal{O}_{V_1}^l + C_{V_2}^l\mathcal{O}_{V_2}^l + C_{S_1}^l\mathcal{O}_{S_1}^l + C_{S_2}^l\mathcal{O}_{S_2}^l + C_T^l\mathcal{O}_T^l], \quad (4)$$

where the four-Fermi operators are defined by

$$\mathcal{O}_{V_1}^l = \bar{c}_L \gamma^\mu b_L \bar{\tau}_L \gamma_\mu \nu_{Ll}, \quad (5)$$

$$\mathcal{O}_{V_2}^l = \bar{c}_R \gamma^\mu b_R \bar{\tau}_L \gamma_\mu \nu_{Ll}, \quad (6)$$

$$\mathcal{O}_{S_1}^l = \bar{c}_L b_R \bar{\tau}_R \nu_{Ll}, \quad (7)$$

$$\mathcal{O}_{S_2}^l = \bar{c}_R b_L \bar{\tau}_R \nu_{Ll}, \quad (8)$$

$$\mathcal{O}_T^l = \bar{c}_R \sigma^{\mu\nu} b_L \bar{\tau}_R \sigma_{\mu\nu} \nu_{Ll}, \quad (9)$$

and C_X^l ($X = V_{1,2}, S_{1,2}, T$) denotes the Wilson coefficient of \mathcal{O}_X^l . Here we assume that the light neutrinos are left-handed.¹ The neutrino flavor is specified by l , and we take all cases of $l = e, \mu$ and τ into account in the contributions of new physics. Since the neutrino flavor is not observed in the experiments of bottom decays, the neutrino mixing does not affect the following argument provided that the Pontecorvo-Maki-Nakagawa-Sakata matrix is unitary. The SM contribution is expressed by the term of $\delta_{l\tau}$ in Eq. (4). We note that the tensor operator with the opposite set of quark chiralities identically vanishes: $\bar{c}_L \sigma^{\mu\nu} b_R \bar{\tau}_R \sigma_{\mu\nu} \nu_{Ll} = 0$.

B. Helicity amplitudes

The helicity amplitude of $\bar{B} \rightarrow M\tau\bar{\nu}$ ($M = D, D^*$) is written as

$$\mathcal{M}_l^{\lambda_\tau, \lambda_M} = \delta_{l\tau} \mathcal{M}_{\text{SM}}^{\lambda_\tau, \lambda_M} + \mathcal{M}_{V_1, l}^{\lambda_\tau, \lambda_M} + \mathcal{M}_{V_2, l}^{\lambda_\tau, \lambda_M} + \mathcal{M}_{S_1, l}^{\lambda_\tau, \lambda_M} + \mathcal{M}_{S_2, l}^{\lambda_\tau, \lambda_M} + \mathcal{M}_{T, l}^{\lambda_\tau, \lambda_M}, \quad (10)$$

where λ_τ is the helicity of the tau lepton, $\lambda_M = s$ indicates the amplitude of $\bar{B} \rightarrow D\tau\bar{\nu}$, and $\lambda_M = \pm 1, 0$ denotes the D^* helicity defined in the B rest frame. The amplitude $\mathcal{M}_{\text{SM}}^{\lambda_\tau, \lambda_M}$ represents the SM contribution and other terms in the right-hand side stand for new physics contributions corresponding to the operators in Eqs. (5)–(9). The SM amplitude is given by [34, 35]

$$\mathcal{M}_{\text{SM}}^{\lambda_\tau, \lambda_M} = \frac{G_F}{\sqrt{2}} V_{cb} \sum_\lambda \eta_\lambda H_{V_1, \lambda}^{\lambda_M} L_{\lambda, \tau}^{\lambda_\tau}, \quad (11)$$

¹ Possibilities to introduce a light right-handed neutrino are discussed in Refs. [32, 33].

and the amplitudes that represent new physics contributions take the following forms:

$$\mathcal{M}_{V_i, l}^{\lambda_\tau, \lambda_M} = \frac{G_F}{\sqrt{2}} V_{cb} C_{V_i}^l \sum_{\lambda} \eta_{\lambda} H_{V_i, \lambda}^{\lambda_M} L_{\lambda, l}^{\lambda_\tau} \quad (i = 1, 2), \quad (12)$$

$$\mathcal{M}_{S_i, l}^{\lambda_\tau, \lambda_M} = -\frac{G_F}{\sqrt{2}} V_{cb} C_{S_i}^l H_{S_i}^{\lambda_M} L_l^{\lambda_\tau} \quad (i = 1, 2), \quad (13)$$

$$\mathcal{M}_{T, l}^{\lambda_\tau, \lambda_M} = -\frac{G_F}{\sqrt{2}} V_{cb} C_T^l \sum_{\lambda, \lambda'} \eta_{\lambda} \eta_{\lambda'} H_{\lambda \lambda'}^{\lambda_M} L_{\lambda \lambda', l}^{\lambda_\tau}, \quad (14)$$

where H 's and L 's are the hadronic and leptonic amplitudes respectively as defined below; $\lambda, \lambda' = \pm, 0, s$ denote the virtual vector boson helicity. The metric factor η_{λ} is given by $\eta_{\pm, 0} = 1$ and $\eta_s = -1$. We treat the contraction of the Lorentz indices in \mathcal{O}_T^l as if two heavy vector bosons are exchanged.

The leptonic amplitudes, $L_{\lambda, l}^{\lambda_\tau}$, $L_l^{\lambda_\tau}$ and $L_{\lambda \lambda', l}^{\lambda_\tau}$ are defined by

$$L_{\lambda, l}^{\lambda_\tau}(q^2, \cos \theta_\tau) = \epsilon_{\mu}(\lambda) \langle \tau(p_\tau, \lambda_\tau) \bar{\nu}_l(p_\nu) | \bar{\tau} \gamma^{\mu} (1 - \gamma_5) \nu_l | 0 \rangle, \quad (15)$$

$$L_l^{\lambda_\tau}(q^2, \cos \theta_\tau) = \langle \tau(p_\tau, \lambda_\tau) \bar{\nu}_l(p_\nu) | \bar{\tau} (1 - \gamma_5) \nu_l | 0 \rangle, \quad (16)$$

$$L_{\lambda \lambda', l}^{\lambda_\tau}(q^2, \cos \theta_\tau) = -i \epsilon_{\mu}(\lambda) \epsilon_{\nu}(\lambda') \langle \tau(p_\tau, \lambda_\tau) \bar{\nu}_l(p_\nu) | \bar{\tau} \sigma^{\mu\nu} (1 - \gamma_5) \nu_l | 0 \rangle, \quad (17)$$

where $\epsilon_{\mu}(\lambda)$ represents the polarization vector of the virtual vector boson, $q^{\mu} = p_B^{\mu} - p_M^{\mu} (= p_{\tau}^{\mu} + p_{\nu}^{\mu})$ is the momentum transfer, and θ_τ denotes the angle between the momentum of the tau lepton and that of the M meson in the rest frame of the leptonic system, to which we refer as the q rest frame [25]. The τ helicity λ_τ is also defined in the q rest frame. The explicit formulae of the leptonic amplitudes are relegated to Appendix A.

The hadronic amplitudes, $H_{V_i, \lambda}^{\lambda_M}$, $H_{S_i}^{\lambda_M}$ and $H_{\lambda \lambda'}^{\lambda_M}$ are defined by

$$H_{V_1, \lambda}^{\lambda_M}(q^2) = \epsilon_{\mu}^*(\lambda) \langle M(p_M, \epsilon(\lambda_M)) | \bar{c} \gamma^{\mu} (1 - \gamma_5) b | \bar{B}(p_B) \rangle, \quad (18)$$

$$H_{V_2, \lambda}^{\lambda_M}(q^2) = \epsilon_{\mu}^*(\lambda) \langle M(p_M, \epsilon(\lambda_M)) | \bar{c} \gamma^{\mu} (1 + \gamma_5) b | \bar{B}(p_B) \rangle, \quad (19)$$

$$H_{S_1}^{\lambda_M}(q^2) = \langle M(p_M, \epsilon(\lambda_M)) | \bar{c} (1 + \gamma_5) b | \bar{B}(p_B) \rangle, \quad (20)$$

$$H_{S_2}^{\lambda_M}(q^2) = \langle M(p_M, \epsilon(\lambda_M)) | \bar{c} (1 - \gamma_5) b | \bar{B}(p_B) \rangle, \quad (21)$$

$$H_{\lambda \lambda'}^{\lambda_M}(q^2) = i \epsilon_{\mu}^*(\lambda) \epsilon_{\nu}^*(\lambda') \langle M(p_M, \epsilon(\lambda_M)) | \bar{c} \sigma^{\mu\nu} (1 - \gamma_5) b | \bar{B}(p_B) \rangle, \quad (22)$$

where $\epsilon(\lambda_M)$ denotes the polarization vector of D^* for $\lambda_M = \pm 1, 0$. The relations $H_{V_1, \lambda}^s = H_{V_2, \lambda}^s$ and $H_{S_1}^s = H_{S_2}^s$ hold because of the parity conservation in the strong interaction. Similarly, we find $H_{S_1}^{\lambda_M} = -H_{S_2}^{\lambda_M}$ for $\lambda_M = \pm 1, 0$.

The hadronic amplitudes of the vector type operators for $\bar{B} \rightarrow D\tau\bar{\nu}$ defined in Eqs. (18) and (19) are represented as

$$H_{V_{1,\pm}}^s(q^2) = H_{V_{2,\pm}}^s(q^2) = 0, \quad (23)$$

$$H_{V_{1,0}}^s(q^2) = H_{V_{2,0}}^s(q^2) = m_B\sqrt{r}(1+r)\frac{\sqrt{w^2-1}}{\sqrt{\hat{q}^2(w)}}V_1(w), \quad (24)$$

$$H_{V_{1,s}}^s(q^2) = H_{V_{2,s}}^s(q^2) = m_B\sqrt{r}(1-r)\frac{w+1}{\sqrt{\hat{q}^2(w)}}S_1(w), \quad (25)$$

and those for $\bar{B} \rightarrow D^*\tau\bar{\nu}$ are

$$H_{V_{1,\pm}}^\pm(q^2) = -H_{V_{2,\mp}}^\mp(q^2) = m_B\sqrt{r}A_1(w)\left[w+1\mp\sqrt{w^2-1}R_1(w)\right], \quad (26)$$

$$H_{V_{1,0}}^0(q^2) = -H_{V_{2,0}}^0(q^2) = m_B\sqrt{r}\frac{w+1}{\sqrt{\hat{q}^2(w)}}A_1(w)[-w+r+(w-1)R_2(w)], \quad (27)$$

$$\begin{aligned} H_{V_{1,s}}^0(q^2) &= -H_{V_{2,s}}^0(q^2) \\ &= \frac{m_B}{2\sqrt{r}}\frac{\sqrt{w^2-1}}{\sqrt{\hat{q}^2(w)}}A_1(w)[-2r(w+1)+(1-r^2)R_2(w)-\hat{q}^2(w)R_3(w)], \end{aligned} \quad (28)$$

$$\text{others} = 0, \quad (29)$$

where $\hat{q}^2(w) = 1+r^2-2rw$, $r = m_M/m_B$, and $w = p_B \cdot p_M/(m_B m_M)$ is the velocity transfer in $\bar{B} \rightarrow M\tau\bar{\nu}$. The form factors, $V_1(w)$, $S_1(w)$, $A_1(w)$ and $R_i(w)$ are defined in Appendix B.

The amplitudes of the scalar type operators are expressed in terms of vector form factors by applying the equations of motion of the quark fields:

$$H_{S_1}^s(q^2) = H_{S_2}^s(q^2) = m_B\sqrt{r}(w+1)S_1(w), \quad (30)$$

$$H_{S_1}^\pm(q^2) = H_{S_2}^\pm(q^2) = 0, \quad (31)$$

$$\begin{aligned} H_{S_1}^0(q^2) &= -H_{S_2}^0(q^2) \\ &= \frac{m_B\sqrt{w^2-1}}{2\sqrt{r}(1+r)}A_1(w)[-2r(w+1)+(1-r^2)R_2(w)-\hat{q}^2(w)R_3(w)]. \end{aligned} \quad (32)$$

Similarly, for the tensor operator, we obtain

$$H_{+-}^s(q^2) = H_{0s}^s(q^2) = m_B\sqrt{r}\frac{\sqrt{w^2-1}}{\hat{q}^2(w)}[-(1+r)^2V_1(w)+2r(w+1)S_1(w)], \quad (33)$$

$$\begin{aligned} H_{\pm 0}^\pm(q^2) &= \pm H_{\pm s}^\pm(q^2) \\ &= \frac{m_B\sqrt{r}}{\sqrt{\hat{q}^2(w)}}A_1(w)\left[\pm(1-r)(w+1)+(1+r)\sqrt{w^2-1}R_1(w)\right], \end{aligned} \quad (34)$$

$$\begin{aligned} H_{+-}^0(q^2) &= H_{0s}^0(q^2) \\ &= \frac{m_B\sqrt{r}}{1+r}A_1(w)\left[-(w+r)(w+1)+(w^2-1)R_3(w)\right], \end{aligned} \quad (35)$$

$$H_{\lambda\lambda'}^{\lambda_M}(q^2) = -H_{\lambda'\lambda}^{\lambda_M}(q^2), \quad (36)$$

and others = 0. A detailed derivation of these hadronic amplitudes is found in Appendix B.

C. Form factors

The form factor $V_1(w)$ is extracted from the experimental data on $\bar{B} \rightarrow D\ell\bar{\nu}$, where $\ell = e, \mu$, provided that the decay process is described by the SM. Employing the following ansatz [36],

$$V_1(w) = V_1(1) [1 - 8\rho_1^2 z + (51.\rho_1^2 - 10.)z^2 - (252.\rho_1^2 - 84.)z^3] , \quad (37)$$

where $z = (\sqrt{w+1} - \sqrt{2})/(\sqrt{w+1} + \sqrt{2})$, the heavy flavor averaging group (HFAG) determines the slope parameter ρ_1^2 as $\rho_1^2 = 1.186 \pm 0.055$ [37].

The form factor $S_1(w)$ does not contribute to the semileptonic B decay into a massless charged lepton. However it reduces to the Isgur-Wise function [38] in the heavy quark limit as well as $V_1(w)$. Accordingly we parametrize it as

$$S_1(w) = [1 + \Delta(w)] V_1(w) , \quad (38)$$

where $\Delta(w)$ denotes the QCD and $1/m_Q$ corrections. Following Refs. [18, 36, 39], we estimate $\Delta(w)$ and give an approximate formula [25]:

$$\Delta(w) = -0.019 + 0.041(w-1) - 0.015(w-1)^2 . \quad (39)$$

As for $\bar{B} \rightarrow D^*\ell\bar{\nu}$, three form factors, $A_1(w)$ and $R_{1,2}(w)$, contribute. They are extracted from experimental data using the following parametrizations:

$$A_1(w) = A_1(1) [1 - 8\rho_{A_1}^2 z + (53\rho_{A_1}^2 - 15)z^2 - (231\rho_{A_1}^2 - 91)z^3] , \quad (40)$$

$$R_1(w) = R_1(1) - 0.12(w-1) + 0.05(w-1)^2 , \quad (41)$$

$$R_2(w) = R_2(1) + 0.11(w-1) - 0.06(w-1)^2 . \quad (42)$$

Eq. (40) is given in Ref. [36] as well as $V_1(w)$. The w dependence of $R_{1,2}$ is estimated by the heavy quark effective theory[39], while $R_1(1)$ and $R_2(1)$ are left as fitting parameters. The HFAG determines these parameters as follows [37]: $\rho_{A_1}^2 = 1.207 \pm 0.026$, $R_1(1) = 1.403 \pm 0.033$ and $R_2(1) = 0.854 \pm 0.020$. The form factor $R_3(w)$ appears only in $\bar{B} \rightarrow D^*\tau\bar{\nu}$ and is estimated by the heavy quark effective theory as [36]

$$R_3(w) = 1 + \Delta_3(w), \quad \Delta_3(w) = 0.22 - 0.052(w-1) + 0.026(w-1)^2 . \quad (43)$$

III. EXPERIMENTAL CONSTRAINTS AND THEORETICAL PREDICTIONS

A. Observables and experimental constraints

There are several measurable quantities affected by new physics operators in $\bar{B} \rightarrow D^{(*)}\tau\bar{\nu}$. We consider the decay rate and the tau longitudinal polarization in $\bar{B} \rightarrow D\tau\bar{\nu}$ and define the following quantities:

$$R(D) = \frac{\Gamma^+(D) + \Gamma^-(D)}{\Gamma(\bar{B} \rightarrow D\ell\bar{\nu})}, \quad P_\tau(D) = \frac{\Gamma^+(D) - \Gamma^-(D)}{\Gamma^+(D) + \Gamma^-(D)}, \quad (44)$$

where $\Gamma^\pm(D)$ represents the decay rate with $\lambda_\tau = \pm 1/2$ as defined in Eq. (C3) and $\Gamma(\bar{B} \rightarrow D\ell\bar{\nu})$ is the total decay rate of $\bar{B} \rightarrow D\ell\bar{\nu}$. The uncertainties that come from V_{cb} and the normalization factor $V_1(1)$ vanish in the above quantities. For $\bar{B} \rightarrow D^*\tau\bar{\nu}$ we also define $R(D^*)$ and $P_\tau(D^*)$ in the same fashion. In addition we introduce the D^* polarization as

$$P_{D^*} = \frac{\Gamma(D_L^*)}{\Gamma(D_L^*) + \Gamma(D_T^*)}, \quad (45)$$

where $D_{L(T)}^*$ represents the longitudinally (transversely) polarized D^* and $\Gamma(D_{L,T}^*)$ are defined in Eq. (C4). The uncertainties in $R(D^*)$, $P_\tau(D^*)$ and P_{D^*} due to V_{cb} and $A_1(1)$ also disappear. The new physics operators are expected to affect these observables in various ways. Thus it is important to study them at the same time in order to distinguish the underlying new physics.

Besides the above integrated quantities, q^2 distributions are potentially sensitive to new physics. As we will illustrate below, the q^2 distribution of $\bar{B} \rightarrow D\tau\bar{\nu}$ decay rate is helpful in discriminating between two scalar operators.

In the following model-independent analysis, we assume that one of the new physics operators in Eq. (4) is dominant except the SM contribution. This assumption allows us to determine the dominant Wilson coefficient from the experimental results of $R(D)$ and $R(D^*)$, and to predict other observables. A situation beyond this assumption is discussed in Sec. V.

In Figs. 1 and 2, we show new physics effects on $R(D^{(*)})$, $P_\tau(D^{(*)})$ and P_{D^*} . The horizontal axis is $|C_X^\tau|$ and three cases of $\delta_X = 0, \pi/2$, and π are shown for illustration, where δ_X is the complex phase of C_X^τ . Effects of $\mathcal{O}_X^{e,\mu}$ are the same as those of \mathcal{O}_X^τ with $\delta_X = \pi/2$ because the new physics contributions do not interfere with the SM amplitudes in these cases. The width of each prediction indicates uncertainties due to the form factors. We include $\pm 100\%$

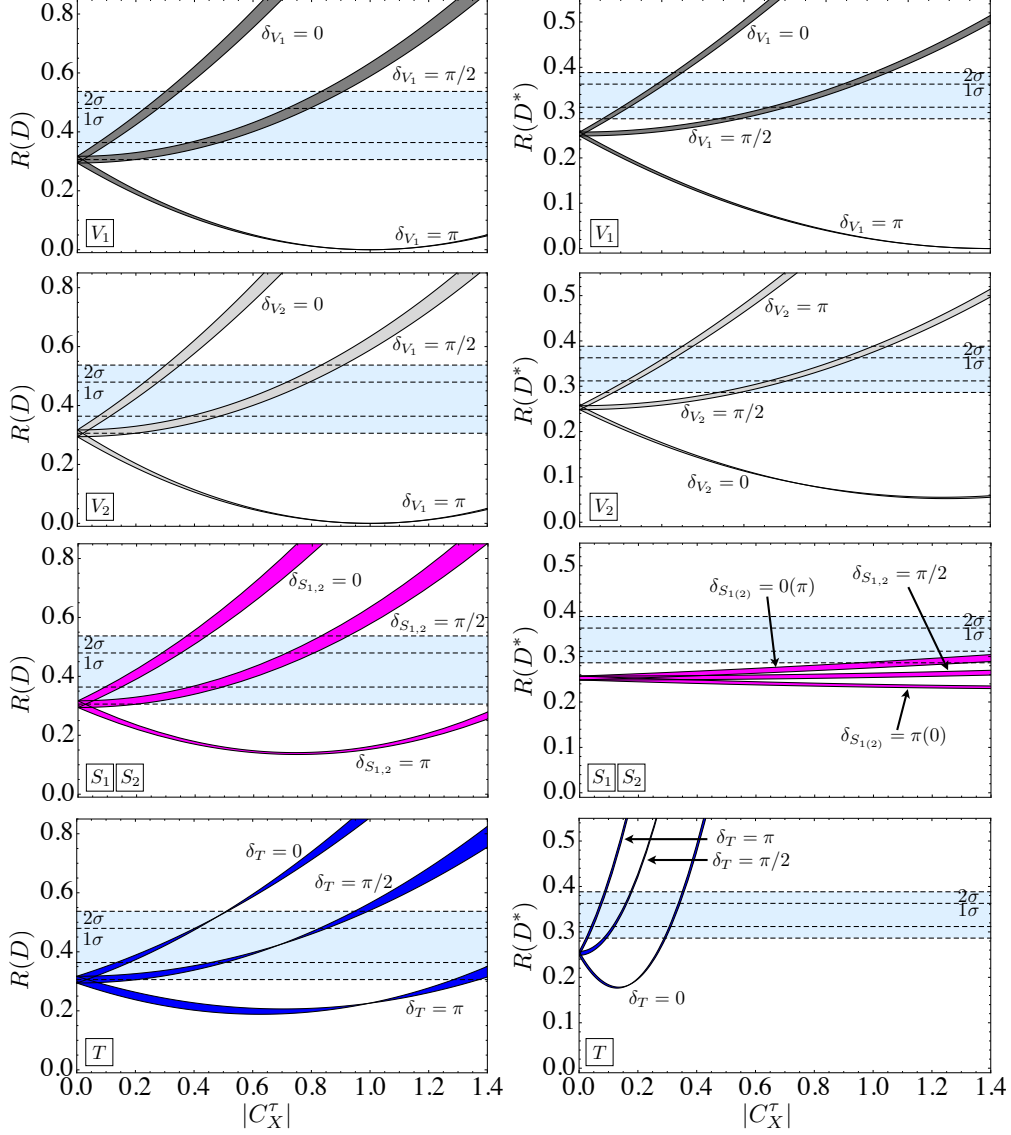


FIG. 1: Predictions on the branching ratios as functions of the absolute value of Wilson coefficient $|C_X^\tau|$ for $X = V_{1,2}, S_{1,2}, T$. The predictions of new physics effects for the operators $\mathcal{O}_X^{e,\mu}$ are given by the lines for $\delta_X = \pi/2$ in these graphs. The light blue horizontal bands represent the experimental values.

errors in the overall magnitudes of $\Delta(w)$ and $\Delta_3(w)$ as uncertainties in addition to the ranges of $\rho_1^2, \rho_{A_1}^2, R_1(1)$ and $R_2(1)$. The horizontal bands with dashed boundaries in Fig. 1 represent the experimental values given in Eq. (2). From these results, we find that the sensitivity to the magnitude of the Wilson coefficient varies depending on each operator. We note that the theoretical uncertainties are sufficiently smaller than the present experimental accuracy. Therefore, we use the central values of the theoretical predictions in the rest of this work

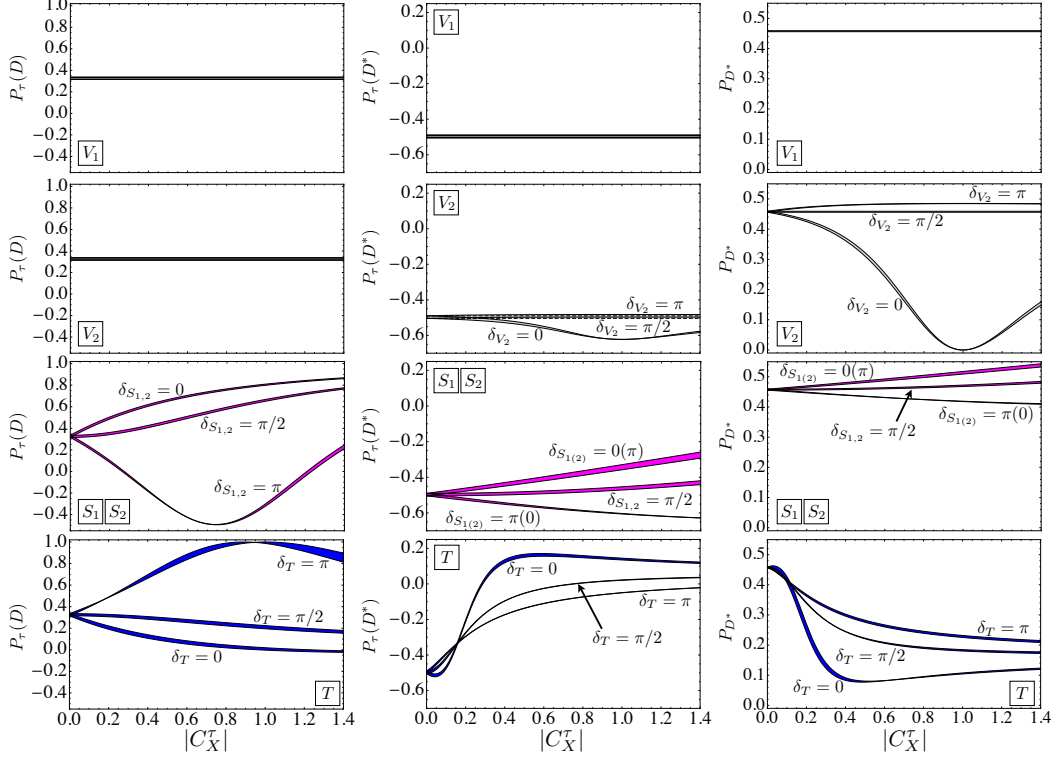


FIG. 2: Predictions on $P_\tau(D)$, $P_\tau(D^*)$ and P_{D^*} as functions of $|C_X^\tau|$ for $X = V_{1,2}, S_{1,2}, T$. The predictions of new physics effects for the operators $\mathcal{O}_X^{e,\mu}$ are given by the lines for $\delta_X = \pi/2$.

unless otherwise stated.

In Fig. 3, the allowed region of the complex Wilson coefficient C_X^τ is shown for each operator \mathcal{O}_X^τ . The vector operators $\mathcal{O}_{V_{1,2}}^\tau$ describe the current experimental results [32]. The operator $\mathcal{O}_{S_1}^\tau$ is unlikely while $\mathcal{O}_{S_2}^\tau$ is favored as is already pointed out in Refs. [32, 40]. In addition, we find that the tensor operator \mathcal{O}_T^τ reasonably explains the current data. We can read the allowed regions of $|C_X^{e,\mu}|$ from that of the pure imaginary C_X^τ , since neither $C_X^{e,\mu}$ nor the pure imaginary C_X^τ interferes with the SM contribution as is mentioned above. Thus, we find no allowed region of the Wilson coefficient within 99% confidence level (C.L.) for $\mathcal{O}_{S_1}^{e,\mu}$ nor $\mathcal{O}_{S_2}^{e,\mu}$. The operators $\mathcal{O}_{V_1}^{e,\mu}$, $\mathcal{O}_{V_2}^{e,\mu}$ and $\mathcal{O}_T^{e,\mu}$ are able to explain the present data.

B. Correlation between $R(D)$ and $R(D^*)$

Since each new physics operator contributes to $R(D)$ and $R(D^*)$ in different ways as seen in Fig. 1, it is useful to examine the correlation between $R(D)$ and $R(D^*)$ for the sake of discrimination of new physics operators. In the left panel of Fig. 4, we show $R(D)$ and

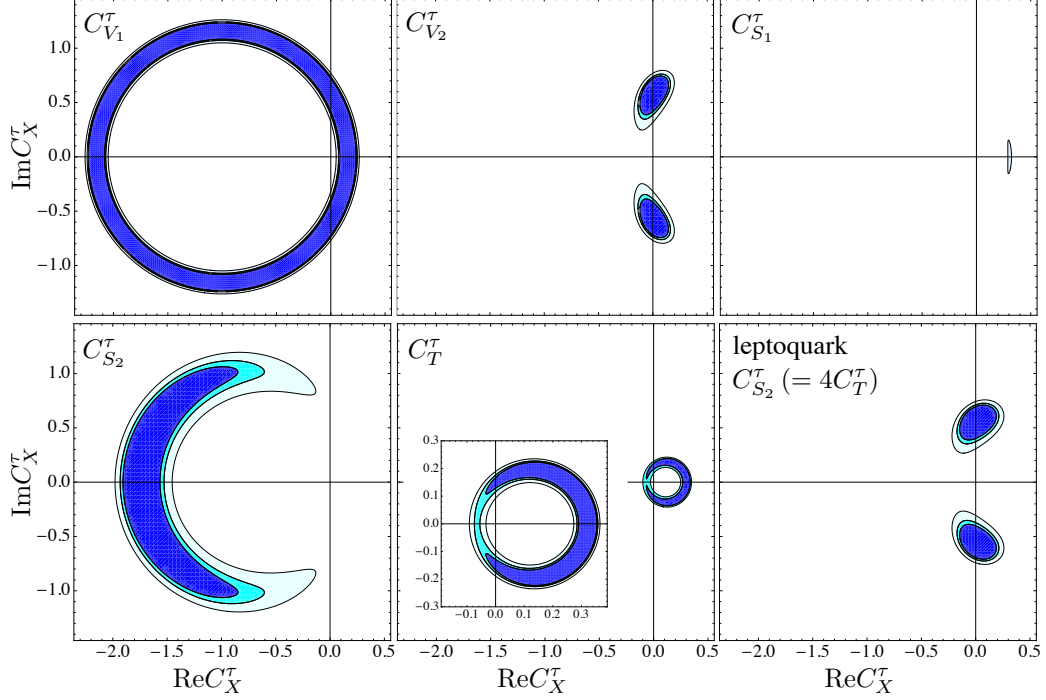


FIG. 3: Constraints on the Wilson coefficient C_X^τ . The allowed regions within 90%(blue), 95%(cyan) and 99%(light blue) C.L. are shown. Allowed regions for $|C_X^{e,\mu}|$ are obtained by those for pure imaginary C_X^τ . The leptiquark panel is mentioned in Sec. V C.

$R(D^*)$ in the presence of the new physics operators for \mathcal{O}_X^τ ($X = V_{1,2}, S_{1,2}$ and T). The shaded regions are predicted by the indicated operators. As is known [15], $R(D)$ is more sensitive to the scalar type operators $\mathcal{O}_{S_1}^\tau$ and $\mathcal{O}_{S_2}^\tau$ than $R(D^*)$. This is due to the angular momentum conservation that gives an extra suppression factor for the vector meson. On the other hand, we find that the tensor type operator \mathcal{O}_T^τ exhibits the opposite behavior, that is, $R(D^*)$ is more sensitive to \mathcal{O}_T^τ than $R(D)$. The vector type operator $\mathcal{O}_{V_1}^\tau$ gives a unique relation between $R(D)$ and $R(D^*)$, since it is just the SM operator and changes only the overall factor. The vector type operator $\mathcal{O}_{V_2}^\tau$ that contains the right-handed quark current covers a wide region in this plane.

The correlations between $R(D)$ and $R(D^*)$ for the lepton flavor violating operators $\mathcal{O}_X^{e,\mu}$ are shown in the right panel of Fig. 4. As these operators do not interfere with the SM one, they always increase $R(D)$ and $R(D^*)$ with different ratios depending on X .

Once a future experiment gives precise values of $R(D)$ and $R(D^*)$, we may exclude some operators depending on the actual experimental values.

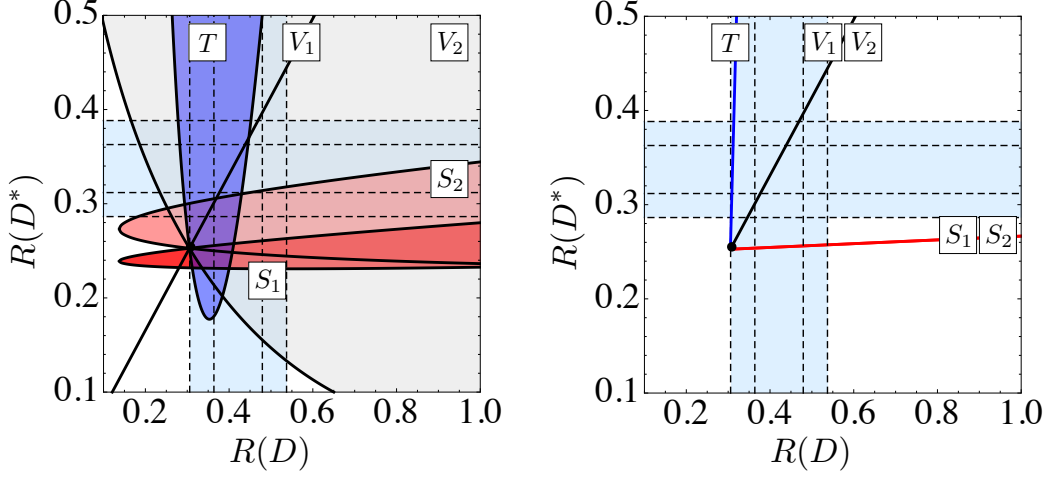


FIG. 4: Correlations between $R(D)$ and $R(D^*)$ in the presence of new physics operators of \mathcal{O}_X^τ (left) and $\mathcal{O}_X^{e,\mu}$ (right) for $X = V_{1,2}, S_{1,2}, T$. The black dot in each panel indicates the SM prediction. The light blue horizontal and vertical bands are the experimental values.

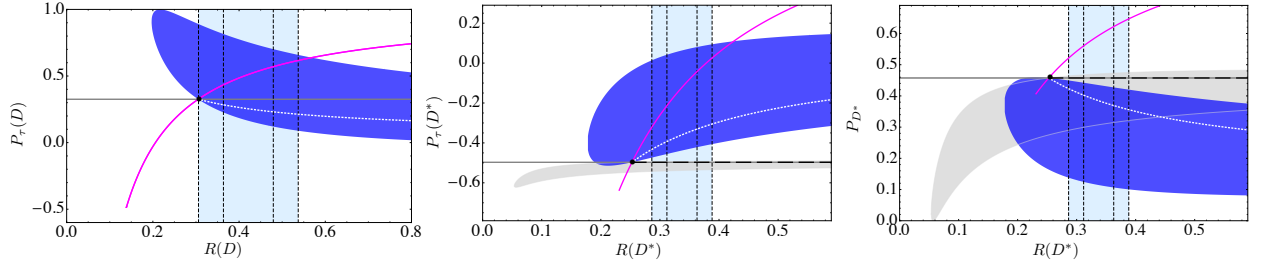


FIG. 5: Correlations between $R(D^*)$ and $P_\tau(D^*)$, and $R(D^*)$ and P_{D^*} in the presence of new physics operators $\mathcal{O}_{V_1}^{e,\mu,\tau}$ (gray horizontal lines), $\mathcal{O}_{V_2}^\tau$ (light gray regions), $\mathcal{O}_{V_2}^{e,\mu}$ (black dashed lines), $\mathcal{O}_{S_{1,2}}^{e,\mu,\tau}$ (magenta curves), \mathcal{O}_T^τ (blue regions) and $\mathcal{O}_T^{e,\mu}$ (white dotted curves). The black dot in each panel indicates the SM prediction. The light blue vertical bands show the experimental constraints.

C. Correlations between decays rates and polarizations

As shown in Fig. 2, polarizations are also useful observables to identify new physics. Here we show correlations between decay rates and polarizations in Fig. 5. The gray horizontal lines represent the correlations for $\mathcal{O}_{V_1}^{e,\mu,\tau}$, the light gray regions (black dashed lines) for $\mathcal{O}_{V_2}^{\tau(e,\mu)}$, the magenta curves for the scalar operators $\mathcal{O}_{S_{1,2}}^{e,\mu,\tau}$, and the blue regions (white dotted curves) for $\mathcal{O}_T^{\tau(e,\mu)}$. The operator $\mathcal{O}_{V_2}^l$ gives the same line as $\mathcal{O}_{V_1}^l$ in $\bar{B} \rightarrow D\tau\bar{\nu}$. The light blue vertical bands show the experimental constraints on $R(D)$ and $R(D^*)$.

We find specific features of the scalar operators in this figure. The polarizations $P_\tau(D^{(*)})$ and P_{D^*} are uniquely related to the corresponding decay rates in the presence of scalar operators, because the scalar operators $\mathcal{O}_{S_1}^l$ and $\mathcal{O}_{S_2}^l$ contribute only to $\Gamma^+(D^{(*)})$ and $\Gamma(D_L^*)$. The definitions of polarizations may be rewritten as

$$[\Gamma^+(D^{(*)}) + \Gamma^-(D^{(*)})] [1 - P_\tau(D^{(*)})] = 2\Gamma^-(D^{(*)}), \quad (46)$$

$$[\Gamma(D_T^*) + \Gamma(D_L^*)] (1 - P_{D^*}) = \Gamma(D_T^*). \quad (47)$$

The right-hand sides of these equations are given solely by the SM contributions, and thus the polarizations are definitely determined by the corresponding decay rates as seen in Fig. 5. These specific correlations are prominent predictions of the scalar type operators, although we cannot discriminate $\mathcal{O}_{S_1}^l$ from $\mathcal{O}_{S_2}^l$ by using these correlations.

As for the other operators, it is apparent that the SM operator $\mathcal{O}_{V_1}^\tau$ and $\mathcal{O}_{V_1}^{e,\mu}$ do not affect the polarizations, while the quark right-handed current $\mathcal{O}_{V_2}^l$ has no effect on the tau polarization in $\bar{B} \rightarrow D\tau\bar{\nu}$ because the axial vector part does not contribute to this process. The operator $\mathcal{O}_{V_2}^{e,\mu}$ in $\bar{B} \rightarrow D^*\tau\bar{\nu}$ and the tensor operator $\mathcal{O}_T^{e,\mu}$ in both the processes predict definite relations between the polarizations and the rates. The operator $\mathcal{O}_{V_2}^\tau$ in $\bar{B} \rightarrow D^*\tau\bar{\nu}$ and the tensor operator \mathcal{O}_T^τ in both the processes have no such specific relations, but the covered regions are rather restricted.

The above correlations that include the polarizations definitely increase the ability to restrict possible new physics. We might uniquely identify the new physics operator by these correlations in some cases. However their usefulness depends on experimental situations as we will see in the next section.

IV. MODEL-INDEPENDENT ANALYSIS OF NEW PHYSICS

In this section, we illustrate several possibilities to restrict or identify new physics using the observables discussed in the previous section and decay distributions. We suppose that $R(D)$ and $R(D^*)$ will be measured more precisely in a future super B factory experiment. Then we will determine the Wilson coefficient C_X^l associated with \mathcal{O}_X^l that is assumed to be dominant except for the SM contribution and predict other observables.

Here we consider the following three cases of $(R(D), R(D^*))$:

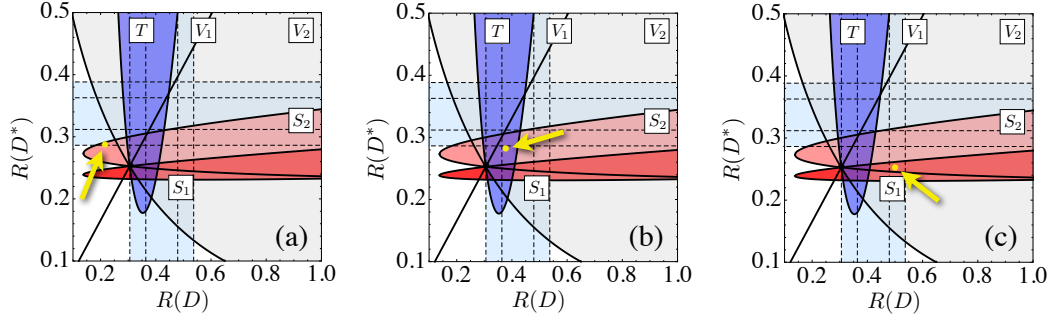


FIG. 6: Three examples for the discrimination of new physics contribution: (a) $R(D) = 0.21$, $R(D^*) = 0.29$, (b) $R(D) = 0.37$, $R(D^*) = 0.28$ and (c) $R(D) = 0.51$, $R(D^*) = 0.25$.

	(a)	(b)			(c)		
$(R(D), R(D^*))$	(0.21, 0.29)	(0.37, 0.28)			(0.51, 0.25)		
X	S_2	S_2	V_2	T	S_1	S_2	V_2
C_X^τ	$-1.20 \pm i 0.18$	$-0.81 \pm i 0.87$	$0.03 \pm i 0.40$	$0.16 \pm i 0.14$	$-0.50 \pm i 1.08$	$0.21 \pm i 0.56$	$0.18 \pm i 0.53$
$P_\tau(D)$	0.02	0.44	0.33	0.22	0.60	0.60	0.33
$P_\tau(D^*)$	-0.30	-0.35	-0.50	-0.26	-0.51	-0.51	-0.50
P_{D^*}	0.53	0.51	0.45	0.32	0.45	0.45	0.44

TABLE I: Predictions for the polarizations in each of three cases.

- (a) (0.21, 0.29) as shown in Fig. 6(a), in which $\mathcal{O}_{S_2}^\tau$ is unambiguously identified as the new physics operator.
- (b) (0.37, 0.28) as shown in Fig. 6(b), in which $\mathcal{O}_{S_2}^\tau$, $\mathcal{O}_{V_2}^\tau$, and \mathcal{O}_T^τ are the candidates for the new physics operator.
- (c) (0.51, 0.25) as shown in Fig. 6(c), in which $\mathcal{O}_{S_1}^\tau$, $\mathcal{O}_{S_2}^\tau$, and $\mathcal{O}_{V_2}^\tau$ are possible.

One of $R(D)$ and $R(D^*)$ is chosen to be within the 2σ range but the other is allowed to deviate more. We note that $\mathcal{O}_X^{e,\mu}$ do not reproduce the assumed sets of $R(D)$ and $R(D^*)$. Table I summarizes the Wilson coefficient and the predicted polarizations for each case.

In the case (a), the dominant new physics operator is uniquely determined to be $\mathcal{O}_{S_2}^\tau$. The polarizations can be used to confirm that the deviation from the SM comes from the operator $\mathcal{O}_{S_2}^\tau$. Furthermore the assumption of one-operator dominance will be tested.

In the case (b), the dominant operator is $\mathcal{O}_{S_2}^\tau$, $\mathcal{O}_{V_2}^\tau$, or \mathcal{O}_T^τ . The predicted values of polarizations vary from operator to operator. We will determine the dominant new physics oper-

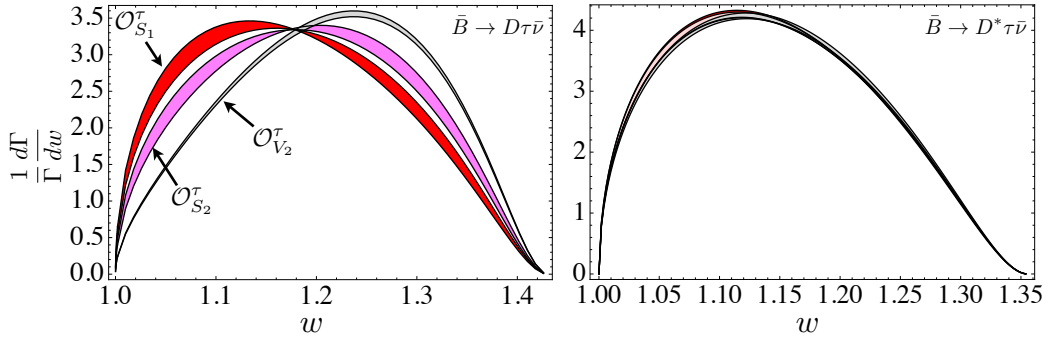


FIG. 7: Distributions of w in $\bar{B} \rightarrow D\tau\bar{\nu}$ and $\bar{B} \rightarrow D^*\tau\bar{\nu}$ for the case (c), where $w = (m_B^2 - m_M^2 - q^2)/(2m_B m_M)$. The red, magenta, and light gray regions represent the distributions in the cases of $\mathcal{O}_{S_1}^\tau$, $\mathcal{O}_{S_2}^\tau$ and $\mathcal{O}_{V_2}^\tau$ respectively, including the theoretical uncertainties as in Sec. III A. The w distributions in $\bar{B} \rightarrow D^*\tau\bar{\nu}$ are almost identical for the three operators.

ator by measuring $P_\tau(D^*)$ for example. Then the one-operator dominance will be checked by looking up other polarizations.

In the case (c), the dominant operator is $\mathcal{O}_{S_1}^\tau$, $\mathcal{O}_{S_2}^\tau$, or $\mathcal{O}_{V_2}^\tau$. The occurrence of $\mathcal{O}_{V_2}^\tau$ is distinguished from that of $\mathcal{O}_{S_1}^\tau$ or $\mathcal{O}_{S_2}^\tau$ by polarizations. Two scalar operators $\mathcal{O}_{S_1}^\tau$ and $\mathcal{O}_{S_2}^\tau$, however, predict the same values of the polarizations as explained in Sec. III C. Under such a situation, q^2 distributions may discriminate between $\mathcal{O}_{S_1}^\tau$ and $\mathcal{O}_{S_2}^\tau$. In Fig. 7, we present q^2 distributions for $\mathcal{O}_{S_1}^\tau$, $\mathcal{O}_{S_2}^\tau$, and $\mathcal{O}_{V_2}^\tau$ in the case (c). We note that the abscissa is $w = (m_B^2 - m_M^2 - q^2)/(2m_B m_M)$ instead of q^2 . The q^2 distribution in $\bar{B} \rightarrow D\tau\bar{\nu}$ turns out to be useful for the discrimination in this case.

V. MODEL ANALYSIS

In this section, we discuss some new physics models which affect $\bar{B} \rightarrow D^{(*)}\tau\bar{\nu}$ based on the results in Sec. III.

A. 2HDMs and MSSM

As known well, the charged Higgs boson in two Higgs doublet models (2HDMs) contributes to $\bar{B} \rightarrow D^{(*)}\tau\bar{\nu}$ and its effect is enhanced in some cases. In order to forbid flavor changing neutral currents (FCNC) at the tree level, a Z_2 symmetry is often imposed in this

	Type I	Type II	Type X	Type Y
ξ_d	$\cot^2 \beta$	$\tan^2 \beta$	-1	-1
ξ_u	$-\cot^2 \beta$	1	1	$-\cot^2 \beta$

TABLE II: Parameters $\xi_{d,u}$ in each type of 2HDMs.

class of models and it results in four distinct 2HDMs [41–44]. Their Yukawa terms are described as

$$\mathcal{L}_Y = -\bar{Q}_L Y_u \tilde{H}_2 u_R - \bar{Q}_L Y_d H_2 d_R - \bar{L}_L Y_\ell H_2 \ell_R + \text{h.c.} \quad (\text{type I}), \quad (48)$$

$$\mathcal{L}_Y = -\bar{Q}_L Y_u \tilde{H}_2 u_R - \bar{Q}_L Y_d H_1 d_R - \bar{L}_L Y_\ell H_1 \ell_R + \text{h.c.} \quad (\text{type II}), \quad (49)$$

$$\mathcal{L}_Y = -\bar{Q}_L Y_u \tilde{H}_2 u_R - \bar{Q}_L Y_d H_2 d_R - \bar{L}_L Y_\ell H_1 \ell_R + \text{h.c.} \quad (\text{type X}), \quad (50)$$

$$\mathcal{L}_Y = -\bar{Q}_L Y_u \tilde{H}_2 u_R - \bar{Q}_L Y_d H_1 d_R - \bar{L}_L Y_\ell H_2 \ell_R + \text{h.c.} \quad (\text{type Y}), \quad (51)$$

where $H_{1,2}$ are Higgs doublets defined as

$$H_i = \begin{pmatrix} h_i^+ \\ (v_i + h_i^0)/\sqrt{2} \end{pmatrix}, \quad \tilde{H}_i = i\sigma_2 H_i, \quad (52)$$

and v_i denotes the vacuum expectation value (VEV) of H_i . The ratio of two VEVs is defined as $\tan \beta = v_2/v_1$ and $v = \sqrt{v_1^2 + v_2^2} = 246 \text{ GeV}$. In type I, all masses of quarks and leptons are given by the VEV of H_2 . In type II, the up-type quarks obtain their masses from H_2 , while the down-type quarks and leptons from H_1 . In type X, H_2 and H_1 are responsible to the quark and lepton masses respectively. The masses of the down-type quarks are given by H_1 and other fermions acquire their masses from H_2 in type Y. Under this definition v_2 generates up-quark masses in any type of Yukawa interaction.

These 2HDMs contain a pair of physical charged Higgs bosons, which contributes to $\bar{B} \rightarrow D^{(*)} \tau \bar{\nu}$. The relevant Wilson coefficients introduced in Eq. (4) are given by

$$C_{S_1}^\tau = -\frac{m_b m_\tau}{m_{H^\pm}^2} \xi_d, \quad C_{S_2}^\tau = -\frac{m_c m_\tau}{m_{H^\pm}^2} \xi_u. \quad (53)$$

where m_{H^\pm} is the mass of the charged Higgs boson. The parameters ξ_d and ξ_u are presented in Table II. To have a sizable charged Higgs effect, $|\xi_{d,u}|$ should be much larger than unity taking the experimental bound on the charged Higgs mass into account. Then the case of $\xi_u = 1$ or $\xi_d = -1$ is not acceptable. The case of $\xi_u = -\cot^2 \beta$ or $\xi_d = \cot^2 \beta$ with $\cot^2 \beta \gg 1$

	Z_u	Z_d	Z_ℓ
Type I	$\frac{\sqrt{2}M_u}{v} \cot \beta - \epsilon_u \sin \beta (1 + \cot^2 \beta)$	$-\frac{\sqrt{2}M_d}{v} \cot \beta + \epsilon_d \sin \beta (1 + \cot^2 \beta)$	$-\frac{\sqrt{2}M_\ell}{v} \cot \beta$
Type II	$\frac{\sqrt{2}M_u}{v} \cot \beta - \epsilon_u \cos \beta (\tan \beta + \cot \beta)$	$\frac{\sqrt{2}M_d}{v} \tan \beta - \epsilon_d \sin \beta (\tan \beta + \cot \beta)$	$\frac{\sqrt{2}M_\ell}{v} \tan \beta$
Type X	$\frac{\sqrt{2}M_u}{v} \cot \beta - \epsilon_u \sin \beta (1 + \cot^2 \beta)$	$-\frac{\sqrt{2}M_d}{v} \cot \beta + \epsilon_d \sin \beta (1 + \cot^2 \beta)$	$\frac{\sqrt{2}M_\ell}{v} \tan \beta$
Type Y	$\frac{\sqrt{2}M_u}{v} \cot \beta - \epsilon_u \cos \beta (\tan \beta + \cot \beta)$	$\frac{\sqrt{2}M_d}{v} \tan \beta - \epsilon_d \sin \beta (\tan \beta + \cot \beta)$	$-\frac{\sqrt{2}M_\ell}{v} \cot \beta$

TABLE III: The matrices $Z_{u,d,\ell}$ in each type of the 2HDM in the presence of the Z_2 breaking terms.

is unnatural since the top Yukawa interaction becomes nonperturbative. The requirement for the top Yukawa interaction to be perturbative results in $\tan \beta \gtrsim 0.4$ [44]. Therefore, $\xi_d = \tan^2 \beta$ in 2HDM of type II is suitable and only $C_{S_1}^\tau$ is enhanced. As we have shown in Sec. III, however, it is difficult to explain the current experimental results by $\mathcal{O}_{S_1}^\tau$ alone. We find that this model is disfavored with about 4σ using the combined experimental values in Eq. (2). This result is consistent with the recent study in Ref. [5].

A possible solution within 2HDMs is to violate the Z_2 symmetry at the cost of FCNC. We introduce the following Z_2 breaking terms in the above four models:

$$\Delta \mathcal{L}_Y = -\bar{Q}_L \epsilon'_u \tilde{H}_1 u_R - \bar{Q}_L \epsilon'_d H_1 d_R + \text{h.c.} \quad (\text{for types I and X}), \quad (54)$$

$$\Delta \mathcal{L}_Y = -\bar{Q}_L \epsilon'_u \tilde{H}_1 u_R - \bar{Q}_L \epsilon'_d H_2 d_R + \text{h.c.} \quad (\text{for types II and Y}), \quad (55)$$

where $\epsilon'_{u,d}$ are 3×3 matrices that control FCNC and the quark fields are those in the weak basis. Writing the Yukawa terms $\mathcal{L}_Y + \Delta \mathcal{L}_Y$ in terms of mass eigenstates, we obtain the following physical charged Higgs interaction terms:

$$\mathcal{L}_{H^\pm} = (\bar{u}_R Z_u^\dagger V_{\text{CKM}} d_L + \bar{u}_L V_{\text{CKM}} Z_d d_R + \bar{\nu}_L Z_\ell \ell_R) H^+ + \text{h.c.}, \quad (56)$$

where V_{CKM} is Cabibbo-Kobayashi-Maskawa (CKM) matrix. Table III shows the expressions of $Z_{u,d,\ell}$, where $M_{u,d,\ell}$ denote the diagonal up-type quark, down-type quark, and lepton mass matrices, and $\epsilon_{u,d}$ represent matrices $\epsilon'_{u,d}$ in the quark mass basis.

The FCNC in the down-quark sector is strongly constrained, so that ϵ_d is negligible in the present analysis. On the other hand, constraints on the FCNC in the up quark sector are rather weak. Recently the 2HDM of type II that allows FCNC in the up quark sector is studied to explain $\bar{B} \rightarrow D^{(*)} \tau \bar{\nu}$ [40]. Table III implies that the operator $\mathcal{O}_{S_2}^\tau$ in types II and X might be significant for large $\tan \beta$. Then the corresponding Wilson coefficient is given

by

$$C_{S_2}^\tau \simeq \frac{V_{tb}}{\sqrt{2}V_{cb}} \frac{vm_\tau}{m_{H^\pm}^2} (\epsilon_u^{tc})^* \sin \beta \tan \beta. \quad (57)$$

As seen in Fig. 3 the current experimental results are described by the 2HDM of the type II or X with FCNC provided that $|\epsilon_u^{tc}| \sim 1$. If this is the case, we expect sizable deviations in polarizations $P_\tau(D^{(*)})$ and P_{D^*} from the SM as designated by the magenta curves in Fig. 5.

The charged Higgs effects on $\bar{B} \rightarrow D^{(*)}\tau\bar{\nu}$ in the minimal supersymmetric standard model (MSSM) are the same as those in the 2HDM of type II at the tree level. Loop corrections induce non-holomorphic terms $\epsilon_{u,d}$ in Eq. (55) [19, 45]. However it seems difficult to enhance ϵ_u^{tc} to be $O(1)$. Thus the sufficient enhancement of $\mathcal{O}_{S_2}^\tau$ is unlikely in MSSM.

B. MSSM with R-parity violation

The R -parity violating (RPV) MSSM [46] may also affect $\bar{B} \rightarrow D^{(*)}\tau\bar{\nu}$ [47–49]. We consider the following superpotential:

$$W_{\text{RPV}} = \frac{1}{2} \lambda_{ijk} L_i L_j E_k^c + \lambda'_{ijk} L_i Q_j D_k^c, \quad (58)$$

where λ_{ijk} and λ'_{ijk} are RPV couplings and i, j, k are generation indices. Apart from the charged Higgs contribution, there are two kinds of diagrams which contribute to $\bar{B} \rightarrow D^{(*)}\tau\bar{\nu}$, that is, the slepton and down squark exchanging diagrams. The corresponding effective Lagrangian is written as

$$\mathcal{L}_{\text{eff}}^{\text{RPV}} = - \sum_{j,k=1}^3 V_{2k} \left[\frac{\lambda_{ij3} \lambda_{jk3}^*}{m_{\tilde{l}_L^j}^2} \bar{c}_L b_R \bar{\tau}_R \nu_L^i + \frac{\lambda'_{i3j} \lambda_{3kj}^*}{m_{\tilde{d}_R^j}^2} \bar{c}_L (\tau^c)_R (\bar{\nu}^c)_R^i b_L \right], \quad (59)$$

where $m_{\tilde{l}_L^j}$ ($m_{\tilde{d}_R^j}$) is the mass of the slepton (down squark) for the j -th generation and V_{ij} is the component of CKM matrix. Here we assume that the slepton and down squark mass matrices are diagonal in the super-CKM basis for simplicity. Using Fierz identity the second term in Eq. (59) is rewritten as

$$\bar{c}_L (\tau^c)_R (\bar{\nu}^c)_R^i b_L = \frac{1}{2} \bar{c}_L \gamma^\mu b_L \bar{\tau}_L \gamma_\mu \nu_L^i. \quad (60)$$

Then, the corresponding coefficients, defined in Eq. (4), are expressed as

$$C_{S_1}^{l_i} = \frac{1}{2\sqrt{2}G_F V_{cb}} \sum_{j,k=1}^3 V_{2k} \frac{\lambda_{ij3} \lambda_{jk3}^*}{m_{\tilde{l}_L^j}^2}, \quad C_{V_1}^{l_i} = \frac{1}{2\sqrt{2}G_F V_{cb}} \sum_{j,k=1}^3 V_{2k} \frac{\lambda'_{i3j} \lambda_{3kj}^*}{2m_{\tilde{d}_R^j}^2}, \quad (61)$$

where $l_1 = e$, $l_2 = \mu$, and $l_3 = \tau$ represent the flavor of the neutrino.

The case that $C_{S_1}^{l_i}$ is dominant contribution is disfavored as discussed in Sec. III. On the other hand $C_{V_1}^{l_i}$ has an allowed region as shown in Fig. 3. We find that $|C_{V_1}^\tau| > 0.08$ and $|C_{V_1}^{e,\mu}| > 0.42$ (90% C.L.) are required to explain the current experimental results. However the same products of RPV couplings as in $C_{V_1}^{l_i}$'s also contribute to $B \rightarrow X_s \nu \bar{\nu}$ [50]. The upper limit of the branching ratio, $\mathcal{B}(B \rightarrow X_s \nu \bar{\nu}) < 6.4 \times 10^{-4}$ (90% C.L.) [51], puts a strong constraint on RPV couplings. It turns out that $|C_{V_1}^{l_i}| < 0.03$ is imposed, which contradicts the above requirement for $\bar{B} \rightarrow D^{(*)} \tau \bar{\nu}$. Thus MSSM with RPV is not likely to be consistent with both $\bar{B} \rightarrow D^{(*)} \tau \bar{\nu}$ and $B \rightarrow X_s \nu \bar{\nu}$ at the same time.

C. Leptoquark models

There are ten possible leptoquark models that respect the symmetry of the SM [52]. Among them, the following leptoquark model is interesting in the sense that the tensor operator is generated [53],

$$\mathcal{L}_{\text{LQ}} = (\lambda_{ij} \bar{Q}^i \varepsilon e_R^j + \lambda'_{ij} \bar{u}_R^i L^j) S_{\text{LQ}}, \quad (62)$$

where S_{LQ} is the scalar leptoquark with $SU(3) \times SU(2) \times U(1)_Y$ quantum number being $(3, 2, 7/6)$. The effective Lagrangian is represented as

$$-\mathcal{L}_{\text{eff}}^{\text{LQ}} = \frac{\lambda_{33}^* \lambda'_{2i}}{m_{S_{\text{LQ}}}^2} (\bar{\tau}_R b_L) (\bar{c}_R \nu_L^i) = -\frac{\lambda_{33}^* \lambda'_{2i}}{2m_{S_{\text{LQ}}}^2} \left(\bar{c}_R b_L \bar{\tau}_R \nu_L^i + \frac{1}{4} \bar{c}_R \sigma^{\mu\nu} b_L \bar{\tau}_R \sigma_{\mu\nu} \nu_L^i \right). \quad (63)$$

Both $\mathcal{O}_{S_2}^{l_i}$ and $\mathcal{O}_T^{l_i}$ appear at the same time, however the Wilson coefficients are related to each other:

$$C_{S_2}^{l_i} = 4C_T^{l_i} = \frac{-1}{2\sqrt{2}G_F V_{cb}} \cdot \frac{\lambda_{33}^* \lambda'_{2i}}{2m_{S_{\text{LQ}}}^2} \simeq -0.6 \left(\frac{\lambda_{33}^* \lambda'_{2i}}{0.4} \right) \left(\frac{500 \text{ GeV}}{m_{S_{\text{LQ}}}} \right)^2. \quad (64)$$

Thus, a similar analysis as the case of one dominant operator can be made.

The bottom right panel in Fig. 3 shows the constraint on the above Wilson coefficient $C_{S_2}^\tau (= 4C_T^\tau)$. We find that the present experimental results are explained with $C_{S_2}^\tau \simeq \pm i 0.6$ or $|C_{S_2}^{e,\mu}| \simeq 0.6$. The relevant mass scale of the leptoquark could be ~ 500 GeV as seen in Eq. (64). In Fig. 8, we show the correlations between decay rates and polarizations in the above leptoquark model. The green regions represent the correlations, $R(D^{(*)})-P_\tau(D^{(*)})$ and $R(D^*)-P_{D^*}$, as in Fig. 5. Taking into account both the experimental constraints on $R(D)$

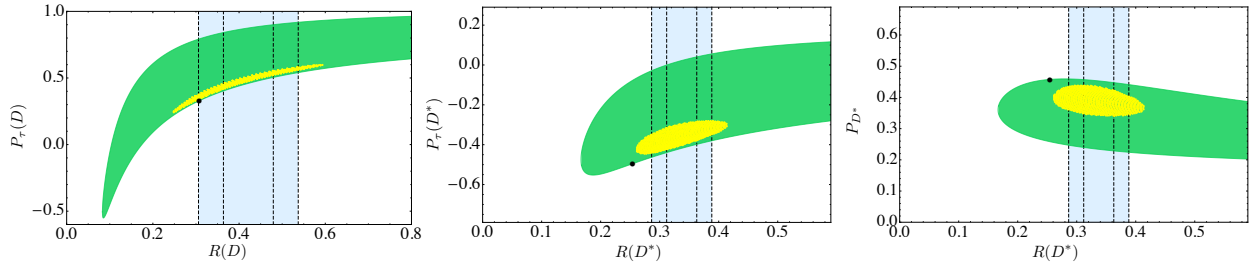


FIG. 8: Correlations between $R(D^{(*)})$ and $P_\tau(D^{(*)})$, and $R(D^*)$ and P_{D^*} in the leptoquark model of Eq. (62) are represented by green regions. Yellow regions indicate the constraints from both the present experimental bounds on $R(D)$ and $R(D^*)$. The black dot in each panel stands for the SM prediction.

and $R(D^*)$ at the same time, we find the present allowed regions at 99% C.L. as shown by the yellow regions.

VI. CONCLUSIONS

We have studied the exclusive semi-tauonic B decays, $\bar{B} \rightarrow D^{(*)}\tau\bar{\nu}$, in the model-independent manner based on the effective Lagrangian including all the possible four-Fermi operators. It has turned out that the current experimental values of $R(D)$ and $R(D^*)$ are not explained by the operator $O_{S_1}^l$ nor $O_{S_2}^{e,\mu}$ alone, while the other operators $O_{S_2}^\tau$, $O_{V_1}^l$, $O_{V_2}^l$, and O_T^l reasonably work under the assumption of one-operator dominance. More precise data that will be given in a future super B factory experiment will allow us to identify the relevant new physics operator among these operators if the deviation from the SM persists. We have pointed out that correlations among observables including the longitudinal tau polarizations, the D^* polarization and q^2 distributions are useful in distinguishing among possible new physics. This observation for the most general effective Lagrangian in Eq. (4) confirms and extends results in the literature for limited new physics cases [25, 27, 29, 31].

Furthermore, we have studied several interesting models that may describe the deviations of $R(D)$ and $R(D^*)$ from the SM based on our model-independent analysis. In 2HDMs without tree-level FCNC and MSSM, only $O_{S_1}^\tau$ could be enhanced and thus are unlikely to explain the deviations, while $O_{S_2}^\tau$ generated in 2HDMs of type II and type X with FCNC might be sizable depending on the magnitude of the $t \rightarrow c$ FCNC parameter. The parameter

region of MSSM with R -parity violation that explains the deviations in $R(D)$ and $R(D^*)$ has turned out to be inconsistent with the experimental bound on $B \rightarrow X_s \nu \bar{\nu}$. The scalar leptoquark model that simultaneously induces $O_{S_2}^l$ and O_T^l describes the experimental data.

In conclusion, $\bar{B} \rightarrow D^{(*)} \tau \bar{\nu}$ is a powerful tool to explore new physics in the charged current. It is important to study combinations of observables including particle polarizations and q^2 distributions as well as the decay rates in order to clarify possible new physics in a model-independent manner. The model-independent analysis gives a firm footing in examining models of new physics.

Acknowledgments

The authors thank A. Tayduganov for his useful comments on the manuscript. This work is supported in part by the Grant-in-Aid for Science Research, Ministry of Education, Culture, Sports, Science and Technology, Japan, under Grants No. 20244037 (M.T.) and No. 248920 (R.W.).

Appendix A: Leptonic amplitudes

In this appendix, we summarize the expressions of the leptonic amplitudes. The vector type leptonic amplitudes are given by

$$L_{\pm}^+ = \pm \sqrt{2} m_{\tau} v \sin \theta_{\tau} , \quad (\text{A1})$$

$$L_0^+ = 2 m_{\tau} v \cos \theta_{\tau} , \quad (\text{A2})$$

$$L_s^+ = -2 m_{\tau} v , \quad (\text{A3})$$

$$L_{\pm}^- = \sqrt{2} \sqrt{q^2} v (1 \pm \cos \theta_{\tau}) , \quad (\text{A4})$$

$$L_0^- = -2 \sqrt{q^2} v \sin \theta_{\tau} , \quad (\text{A5})$$

$$L_s^- = 0 , \quad (\text{A6})$$

where $v = \sqrt{1 - m_{\tau}^2/q^2}$. The scalar type leptonic amplitudes are written as

$$L^+ = -2 \sqrt{q^2} v , \quad (\text{A7})$$

$$L^- = 0 . \quad (\text{A8})$$

The tensor type leptonic amplitudes are

$$L_{\lambda\lambda}^{\pm} = 0 , \quad (\text{A9})$$

$$L_{0\pm}^+ = -L_{\pm 0}^+ = -\sqrt{2}\sqrt{q^2}v \sin \theta_{\tau} , \quad (\text{A10})$$

$$L_{+-}^+ = -L_{-+}^+ = L_{s0}^+ = -L_{0s}^+ = 2\sqrt{q^2}v \cos \theta_{\tau} , \quad (\text{A11})$$

$$L_{\pm s}^+ = -L_{s\pm}^+ = \mp\sqrt{2}\sqrt{q^2}v \sin \theta_{\tau} , \quad (\text{A12})$$

$$L_{0\pm}^- = -L_{\pm 0}^- = \mp\sqrt{2}m_{\tau}v(1 \pm \cos \theta_{\tau}) , \quad (\text{A13})$$

$$L_{+-}^- = -L_{-+}^- = L_{s0}^- = -L_{0s}^- = -2m_{\tau}v \sin \theta_{\tau} , \quad (\text{A14})$$

$$L_{\pm s}^- = -L_{s\pm}^- = -\sqrt{2}m_{\tau}v(1 \pm \cos \theta_{\tau}) . \quad (\text{A15})$$

The subscript l that represents the neutrino flavor is omitted for brevity.

Appendix B: Form factors and hadronic amplitudes

Here, we show the definitions of the relevant form factors and the hadronic amplitudes in $\bar{B} \rightarrow D^{(*)}\tau\bar{\nu}$. We also discuss how to evaluate the scalar and tensor form factors by using the equations of motion.

1. Vector and axial vector operators

We define the form factors of the vector and axial vector operators in $\bar{B} \rightarrow D^{(*)}\tau\bar{\nu}$ as,

$$\langle D(p_D) | \bar{c}\gamma^{\mu}b | \bar{B}(p_B) \rangle = \sqrt{m_B m_D} [h_+(w)(v + v')^{\mu} + h_-(w)(v - v')^{\mu}] , \quad (\text{B1})$$

$$\langle D^*(p_{D^*}, \epsilon) | \bar{c}\gamma^{\mu}b | \bar{B}(p_B) \rangle = i\sqrt{m_B m_{D^*}} h_V(w) \epsilon^{\mu\nu\rho\sigma} \epsilon_{\nu}^* v'_{\rho} v_{\sigma} , \quad (\text{B2})$$

$$\begin{aligned} \langle D^*(p_{D^*}, \epsilon) | \bar{c}\gamma^{\mu}\gamma^5 b | \bar{B}(p_B) \rangle &= \sqrt{m_B m_{D^*}} [h_{A_1}(w)(w + 1)\epsilon^{*\mu} \\ &\quad - (\epsilon^* \cdot v)(h_{A_2}(w)v^{\mu} + h_{A_3}(w)v'^{\mu})] , \end{aligned} \quad (\text{B3})$$

where $v = p_B/m_B, v' = p_{D^*}/m_{D^*}$, and $w = v \cdot v'$ in $\bar{B} \rightarrow D^{(*)}\tau\bar{\nu}$. The polarization vector of D^* is indicated as ϵ^{μ} .

Using these definitions, the hadronic amplitudes defined in Eqs. (18) and (19) are repre-

sented as

$$H_{V_1,\pm}^s = H_{V_2,\pm}^s = 0, \quad (\text{B4})$$

$$H_{V_1,0}^s = H_{V_2,0}^s = m_B \sqrt{r} \frac{\sqrt{w^2 - 1}}{\sqrt{\hat{q}^2(w)}} [(1+r)h_+(w) - (1-r)h_-(w)], \quad (\text{B5})$$

$$H_{V_1,s}^s = H_{V_2,s}^s = m_B \sqrt{r} \frac{1}{\sqrt{\hat{q}^2(w)}} [(1-r)(w+1)h_+(w) - (1+r)(w-1)h_-(w)], \quad (\text{B6})$$

in $\bar{B} \rightarrow D\tau\bar{\nu}$ and those in $\bar{B} \rightarrow D^*\tau\bar{\nu}$ are given by

$$\begin{aligned} H_{V_1,\pm}^\pm &= -H_{V_2,\mp}^\mp \\ &= m_B \sqrt{r} \left[(w+1)h_{A_1}(w) \mp \sqrt{w^2 - 1}h_V(w) \right], \end{aligned} \quad (\text{B7})$$

$$\begin{aligned} H_{V_1,0}^0 &= -H_{V_2,0}^0 \\ &= m_B \sqrt{r} \frac{w+1}{\sqrt{\hat{q}^2(w)}} [-(w-r)h_{A_1}(w) + (w-1)(rh_{A_2}(w) + h_{A_3}(w))], \end{aligned} \quad (\text{B8})$$

$$\begin{aligned} H_{V_1,s}^0 &= -H_{V_2,s}^0 \\ &= m_B \sqrt{r} \frac{\sqrt{w^2 - 1}}{\sqrt{\hat{q}^2(w)}} [-(w+1)h_{A_1}(w) + (1-rw)h_{A_2}(w) + (w-r)h_{A_3}(w)], \end{aligned} \quad (\text{B9})$$

$$\text{others} = 0. \quad (\text{B10})$$

In the heavy quark limit, we obtain $h_+(w) = h_{A_{1,3}}(w) = h_V(w) = \xi(w)$ and $h_-(w) = h_{A_2}(w) = 0$ where $\xi(w)$ is Isgur-Wise function [38]. In order to evaluate these form factors by using dispersion relations and the heavy quark effective theory, it is convenient to redefine the form factors as follows [36]:

$$V_1(w) = h_+(w) - \frac{1-r}{1+r}h_-(w), \quad (\text{B11})$$

$$S_1(w) = h_+(w) - \frac{1+r}{1-r} \frac{w-1}{w+1}h_-(w), \quad (\text{B12})$$

$$A_1(w) = h_{A_1}(w), \quad (\text{B13})$$

$$R_1(w) = \frac{h_V(w)}{h_{A_1}(w)}, \quad (\text{B14})$$

$$R_2(w) = \frac{h_{A_3}(w) + rh_{A_2}(w)}{h_{A_1}(w)}, \quad (\text{B15})$$

$$R_3(w) = \frac{h_{A_3}(w) - rh_{A_2}(w)}{h_{A_1}(w)}. \quad (\text{B16})$$

2. Scalar and pseudo-scalar operators

For the scalar and pseudo-scalar operators, the form factors are defined as

$$\langle D(p_D) | \bar{c}b | \bar{B}(p_B) \rangle = \sqrt{m_B m_D} (w+1) h_S(w), \quad (\text{B17})$$

$$\langle D^*(p_{D^*}, \epsilon) | \bar{c} \gamma^5 b | \bar{B}(p_B) \rangle = -\sqrt{m_B m_{D^*}} (\epsilon^* \cdot v) h_P(w), \quad (\text{B18})$$

and then the hadronic amplitudes in Eqs. (20) and (21) are represented as

$$H_{S_1}^s = H_{S_2}^s = m_B \sqrt{r} (w+1) h_S(w), \quad (\text{B19})$$

in $\bar{B} \rightarrow D\tau\bar{\nu}$, and

$$H_{S_1}^\pm = H_{S_2}^\pm = 0, \quad (\text{B20})$$

$$H_{S_1}^0 = -H_{S_2}^0 = -m_B \sqrt{r} \sqrt{w^2 - 1} h_P(w), \quad (\text{B21})$$

in $\bar{B} \rightarrow D^*\tau\bar{\nu}$.

Using the quark equations of motion we obtain

$$i\partial_\mu (\bar{c} \gamma^\mu b) = (m_b - m_c) \bar{c} b, \quad (\text{B22})$$

$$i\partial_\mu (\bar{c} \gamma^\mu \gamma^5 b) = -(m_b + m_c) \bar{c} \gamma^5 b, \quad (\text{B23})$$

which lead to the following relations among form factors:

$$\begin{aligned} h_S(w) &= h_+(w) - \frac{1+r}{1-r} \frac{w-1}{w+1} h_-(w) + O\left(\frac{\Lambda^2}{m_Q^2}\right) \\ &= S_1(w) + O\left(\frac{\Lambda^2}{m_Q^2}\right), \end{aligned} \quad (\text{B24})$$

$$\begin{aligned} h_P(w) &= \frac{1}{1+r} [(w+1)h_{A_1}(w) + (rw-1)h_{A_2}(w) - (w-r)h_{A_3}(w)] + O\left(\frac{\Lambda}{m_Q}\right) \\ &= \frac{A_1(w)}{1+r} \left[w+1 - \frac{1-r^2}{2r} R_2(w) + \frac{\hat{q}^2(w)}{2r} R_3(w) \right] + O\left(\frac{\Lambda}{m_Q}\right), \end{aligned} \quad (\text{B25})$$

where we have used $m_{B(M)} = m_{b(c)} + \Lambda + O(\Lambda^2/m_{b(c)})$. The absence of $1/m_Q$ corrections in Eq. (B24) is confirmed by the heavy quark expansion without resorting to the equations of motion. Thus we employ $h_S(w) = S_1(w) = [1 + \Delta(w)] V_1(w)$, where $\Delta(w)$ involves the $1/m_Q$ corrections. On the other hand, there exist unknown $1/m_Q$ corrections in Eq. (B25). We ignore them, but use the axial vector form factors $A_1(w)$ and $R_{2,3}(w)$ including $1/m_Q$

corrections as described in Sec. II C. The $1/m_Q$ corrections in $R_2(w)$ are necessary to evaluate the rate of $\bar{B} \rightarrow D^* \ell \bar{\nu}$, because the experimental determination of the slope parameter $\rho_{A_1}^2$ assumes these corrections [37]. As for $R_3(w)$, since it does not contribute to $\bar{B} \rightarrow D^* \ell \bar{\nu}$ and no experimental data are available, we use the theoretical estimation by the heavy quark effective theory with $\pm 100\%$ error in $1/m_Q$ corrections.

3. Tensor operator

The form factors of the tensor operator are defined as

$$\langle D(p_D) | \bar{c} \sigma^{\mu\nu} b | \bar{B}(p_B) \rangle = -i \sqrt{m_B m_D} h_T(w) (v^\mu v'^\nu - v^\nu v'^\mu), \quad (\text{B26})$$

$$\begin{aligned} \langle D^*(p_{D^*}, \epsilon) | \bar{c} \sigma^{\mu\nu} b | \bar{B}(p_B) \rangle = & -\sqrt{m_B m_{D^*}} \varepsilon^{\mu\nu\rho\sigma} \left[h_{T_1}(w) \epsilon_\rho^* (v + v')_\sigma + h_{T_2}(w) \epsilon_\rho^* (v - v')_\sigma \right. \\ & \left. + h_{T_3}(w) (\epsilon^* \cdot v) (v + v')_\rho (v - v')_\sigma \right], \end{aligned} \quad (\text{B27})$$

where $\sigma^{\mu\nu} = (i/2) [\gamma^\mu, \gamma^\nu]$ and $\varepsilon^{0123} = -1$. The amplitudes corresponding to the operator $\bar{c} \sigma^{\mu\nu} \gamma_5 b$ are given by the following identity,

$$\sigma^{\mu\nu} \gamma_5 = -\frac{i}{2} \varepsilon^{\mu\nu\alpha\beta} \sigma_{\alpha\beta}. \quad (\text{B28})$$

With the above form factors, the hadronic amplitudes in Eq. (22) are represented as

$$H_{+-}^s(q^2) = H_{0s}^s(q^2) = -m_B \sqrt{r} \sqrt{w^2 - 1} h_T(w), \quad (\text{B29})$$

$$\begin{aligned} H_{\pm 0}^\pm(q^2) &= \pm H_{\pm s}^\pm(q^2) \\ &= \pm m_B \sqrt{r} \frac{1 - rw \pm r \sqrt{w^2 - 1}}{\sqrt{\hat{q}^2(w)}} \\ &\quad \times \left[h_{T_1}(w) + h_{T_2}(w) + (w \pm \sqrt{w^2 - 1})(h_{T_1}(w) - h_{T_2}(w)) \right], \end{aligned} \quad (\text{B30})$$

$$\begin{aligned} H_{+-}^0(q^2) &= H_{0s}^0(q^2) \\ &= -m_B \sqrt{r} \left[(w + 1) h_{T_1}(w) + (w - 1) h_{T_2}(w) + 2(w^2 - 1) h_{T_3}(w) \right], \end{aligned} \quad (\text{B31})$$

$$H_{\lambda\lambda'}^{\lambda_M}(q^2) = -H_{\lambda'\lambda}^{\lambda_M}(q^2), \quad (\text{B32})$$

$$\text{others} = 0. \quad (\text{B33})$$

As in the case of the scalar type operators, the equations of motion lead to

$$\partial_\mu (\bar{c} \sigma^{\mu\nu} b) = -(m_b + m_c) \bar{c} \gamma^\nu b - (i \partial^\nu \bar{c}) b + \bar{c} (i \partial^\nu b), \quad (\text{B34})$$

and we obtain

$$h_T(w) = h_+(w) - \frac{1+r}{1-r}h_-(w) + O\left(\frac{\Lambda}{m_Q}\right), \quad (\text{B35})$$

$$h_{T_1}(w) = \frac{1}{2\hat{q}^2(w)} [(1-r)^2(w+1)h_{A_1}(w) - (1+r)^2(w-1)h_V(w)] + O\left(\frac{\Lambda}{m_Q}\right), \quad (\text{B36})$$

$$h_{T_2}(w) = \frac{(1-r^2)(w+1)}{2\hat{q}^2(w)} [h_{A_1}(w) - h_V(w)] + O\left(\frac{\Lambda}{m_Q}\right), \quad (\text{B37})$$

$$h_{T_3}(w) = -\frac{1}{2(1+r)\hat{q}^2(w)} [2r(w+1)h_{A_1}(w) - \hat{q}^2(w)(rh_{A_2}(w) - h_{A_3}(w)) - (1+r)^2h_V(w)] + O\left(\frac{\Lambda}{m_Q}\right). \quad (\text{B38})$$

We find $h_T(w) = h_{T_1}(w) = \xi(w)$ and $h_{T_2}(w) = h_{T_3}(w) = 0$ in the heavy quark limit. Similarly to the case of the scalar type operators, we ignore the unknown $1/m_Q$ corrections in the right-hand sides, and employ the vector and axial vector form factors with the $1/m_Q$ corrections.

Appendix C: Decay rates

The differential decay rate $\bar{B} \rightarrow M\tau\bar{\nu}$ is represented as

$$d\Gamma_{\lambda_M}^{\lambda_\tau} = \frac{1}{2m_B} \sum_l \left| \mathcal{M}_l^{\lambda_\tau, \lambda_M}(q^2, \cos\theta_\tau) \right|^2 d\Phi_3, \quad (\text{C1})$$

where the three-body phase space $d\Phi_3$ is given by

$$d\Phi_3 = \frac{\sqrt{Q_+Q_-}}{256\pi^3m_B^2} \left(1 - \frac{m_\tau^2}{q^2}\right) dq^2 d\cos\theta_\tau, \quad (\text{C2})$$

and $Q_\pm = (m_B \pm m_M)^2 - q^2$. Several decay rates used in the main text are obtained by integrating Eq. (C1) over q^2 and $\cos\theta_\tau$. For notational simplicity, we define the following quantities:

$$\Gamma^\pm(D) = \Gamma_s^{\pm 1/2}, \quad \Gamma^\pm(D^*) = \sum_{\lambda_M=\pm 1,0} \Gamma_{\lambda_M}^{\pm 1/2}, \quad (\text{C3})$$

$$\Gamma(D_T^*) = \sum_{\lambda_M=\pm 1} \sum_{\lambda_\tau} \Gamma_{\lambda_M}^{\lambda_\tau}, \quad \Gamma(D_L^*) = \sum_{\lambda_\tau} \Gamma_0^{\lambda_\tau}. \quad (\text{C4})$$

[1] For instance, R. E. Marshak, Riazuddin and C. P. Ryan, *THEORY OF WEAK INTERACTIONS*, John Wiley & Sons (1969).

- [2] B. Aubert *et al.* (BABAR Collaboration), Phys. Rev. D **81**, 051101(R) (2010). arXiv:0809.4027 [hep-ex].
- [3] I. Adachi *et al.* (Belle Collaboration), arXiv:0809.3834 [hep-ex].
- [4] B. Aubert *et al.* (BABAR Collaboration), Phys. Rev. D **79**, 092002 (2009). arXiv:0902.2660 [hep-ex].
- [5] J. P. Lees *et al.*, Phys. Rev. Lett. **109**, 101802 (2012). arXiv:1205.5442 [hep-ex].
- [6] A. Matyjka *et al.* (Belle Collaboration), Phys. Rev. Lett. **99**(2007)191807. arXiv:0706.4429 [hep-ex].
- [7] I. Adachi *et al.* (Belle Collaboration), arXiv:0910.4301 [hep-ex].
- [8] A. Bozek *et al.* (Belle Collaboration), Phys. Rev. D **82**, 072005 (2010). arXiv:1005.2302 [hep-ex].
- [9] G. Aad *et al.* (ATLAS Collaboration), Phys. Lett. B **716**, 1 (2012).
- [10] S. Chatrchyan *et al.* (CMS Collaboration), Phys. Lett. B **716**, 30 (2012).
- [11] For a review, *e.g.*, J. F. Gunion, H. E. Haber, G. Kane and S. Dawson, *The Higgs Hunter's Guide*, Frontiers in Physics series, Addison-Wesley (1990).
- [12] See, *e.g.* H. P. Nilles, Phys. Rept. **110**, 1 (1984); S. P. Martin, *A Supersymmetry Primer*, in *Perspectives on Supersymmetry II*, G.L. Kane (ed.), World Scientific (2010). hep-ph/9709356.
- [13] B. Grzadkowski and W. S. Hou, Phys. Lett. B **283**, 427 (1992).
- [14] W. S. Hou, Phys. Rev. D **48**, 2342 (1993).
- [15] M. Tanaka, Z. Phys. C **67**, 321 (1995). hep-ph/9411405.
- [16] K. Kiers and A. Soni, Phys. Rev. D **56**, 5786 (1997). hep-ph/9706337.
- [17] T. Miura and M. Tanaka, hep-ph/0109244.
- [18] T. Miki, T. Miura and M. Tanaka, hep-ph/0210051.
- [19] H. Itoh, S. Komine and Y. Okada, Prog. Theor. Phys. **114**, 179, 2005. hep-ph/0409228.
- [20] C.-H. Chen and C.-Q. Geng, Phys. Rev. D **71**, 077501 (2005). hep-ph/0503123.
- [21] C.-H. Chen and C.-Q. Geng, JHEP 0610, **053**, 2006. hep-ph/0608166.
- [22] U. Nierste, S. Trine and S. Westhoff, Phys. Rev. D **78**, 015006 (2008). arXiv:0801.4938 [hep-ph].
- [23] S. Trine, Talk given at 34th International Conference on High Energy Physics (ICHEP 2008), Philadelphia, Pennsylvania, 30 Jul - 5 Aug 2008. arXiv:0810.3633 [hep-ph].
- [24] J. F. Kamenik and F. Mescia, Phys. Rev. D **78**, 014003 (2008). arXiv:0802.3790 [hep-ph].

- [25] M. Tanaka and R. Watanabe, Phys. Rev. D **82**, 034027 (2010).
- [26] J. A. Bailey, *et al.*, Phys. Rev. Lett. **109**, 071802 (2012). arXiv:1206.4992 [hep-ph].
- [27] S. Fajfer, J. F. Kamenik and I. Nišandžić, Phys. Rev. D **85**, 094025 (2012). arXiv:1203.2654 [hep-ph].
- [28] Y. Sakaki and H. Tanaka, arXiv:1205.4908 [hep-ph].
- [29] A. Datta, M. Duraissamy, and D. Ghosh, Phys. Rev. D **86**, 034027 (2012). arXiv:1206.3760 [hep-ph].
- [30] D. Birevica, N. Kosnikb, and A. Tayduganov Phys. Lett. B **716**, 208 (2012). arXiv:1206.4977 [hep-ph].
- [31] A. Celis, M. Jung, X.-Q. Li, and A. Pich, arXiv:1210.8443 [hep-ph].
- [32] S. Fajfer, J. F. Kamenik, I. Nišandžić and J. Zupan, Phys. Rev. Lett. **109**, 161801 (2012). arXiv:1206.1872 [hep-ph].
- [33] X.-G. He and G. Valencia, arXiv:1211.0348 [hep-ph].
- [34] K. Hagiwara, A.D. Martin, and M.F. Wade, Nucl. Phys. **B327**, 569 (1989).
- [35] K. Hagiwara, A.D. Martin, and M.F. Wade, Z. Phys. **C46**, 299 (1990).
- [36] I. Caprini, L. Lellouch, and M. Neubert, Nucl. Phys. **B530**, 153 (1998). hep-ph/9712417.
- [37] The Heavy Flavor Averaging Group, <http://www.slac.stanford.edu/xorg/hfag/>, 2011.
- [38] N. Isgur and M.B. Wise, Phys. Lett **B232**, 113 (1989); Phys. Lett **B237**, 527 (1990).
- [39] M. Neubert, Phys. Rep. **245**, 259 (1994). hep-ph/9306320.
- [40] A. Crivellin, C. Greub, and A. Kokulu, Phys. Rev. D **86**, 054014 (2012). arXiv:1206.2634 [hep-ph].
- [41] V. D. Barger, J. L. Hewett, and R. J. N. Phillips, Phys. Rev. D **41**, 3421 (1990).
- [42] Y. Grossman, Nucl. Phys. B **426**, 355 (1994).
- [43] A. G. Akeroyd and W. J. Stirling, Nucl. Phys. B **447**, 3 (1995); A. G. Akeroyd, Phys. Lett. B **377**, 95 (1996); J. Phys. G **24**, 1983 (1998).
- [44] M. Aoki, S. Kanemura, K. Tsumura, and K. Yagyu, Phys. Rev. D **80**, 015017, 2009.
- [45] A. Crivellin, Phys. Rev. D **83**, 056001 (2011).
- [46] R. Barbier *et al.*, Phys. Rep. **420**, 1 (2005).
- [47] J. Erler, J. L. Feng, and N. Polonsky, Phys. Rev. Lett. **78**, 3063 (1997).
- [48] M. Chemtob, Prog. Part. Nucl. Phys. **54**, 71 (2005).
- [49] N. G. Deshpande, and A. Menon, arXiv:1208.4134 [hep-ph].

- [50] Y. Grossman, Z. Ligeti, and E. Nardi, Nucl. Phys. **B465**, 369 (1996), Nuclear Phys. **B480**, 753 (1996).
- [51] R. Barate *et al.* (ALEPH Collaboration), Eur. Phys. J. C **19**, 213 (2001).
- [52] W. Buchmuller, R. Ruckl, and D. Wyler, Phys. Lett. B **191**, 442 (1987); Phys. Lett. B **448**, 320(E) (1999).
- [53] J. P. Lee, Phys. Lett. B **526**, 61 (2002).